Wannier Representation of Intraband High-Order Harmonic Generation

F. Catoire, H. Bachau, Z. Wang, C. Blaga, P. Agostini, and L. F. DiMauro

Phys. Rev. Lett. **121**, 143902 — Published 5 October 2018

DOI: 10.1103/PhysRevLett.121.143902

Wannier representation of intraband high-order harmonic generation

F. Catoire* and H. Bachau
Centre des Lasers Intenses et Applications CNRS-CEA-Univsersité de Bordeaux,
351 Cours de la Libération, Talence F-33405, France

Z. Wang, C. Blaga, P. Agostini, and L. Dimauro
Department of Physics, The Ohio State University, Columbus, Ohio 43210, USA

We investigate the harmonic generation induced by the interaction of a mid-IR laser field with a solid target. The harmonic spectra is composed of the contribution of two processes interpreted as interband and intraband transitions. The interband process corresponds to the recombination from an upper band, populated during the laser interaction, to a lower band. The intraband process originates from nonlinear processes of the current in individual bands. In this Letter, we develop a theory based on Wannier states and reveal in depth the underlying physics of intraband dynamics. In particular, this approach highlights the determinant role of transitions between different lattice wells. Furthermore our approach provides quantitative predictions concerning high-order harmonic energy cutoffs, harmonic yields and emission times.

High-order-harmonic generation (HHG) has first been observed in atoms and theoretically described by the so-called three-step model [1–3]. First, an electron wave packet is released into the continuum near the maximum of the linearly polarized IR laser electric field. The subsequent wave packet evolves under the influence of the oscillating laser field and thus acquires kinetic energy. Finally, as the electric field reverses its direction, the wave packet has a probability to come back in the vicinity of the parent ion and to recombine emitting the energy gained as a photon in the UV-XUV range. From semi-classical analysis the energy gained at recombination spans from 0 to a maximum of $3.17U_p$ leading to a cut-off in the harmonic spectra. The ponderomotive energy U_p is given by $U_p = \frac{I}{4\omega_0^2}$ which is expressed in atomic units with I the peak laser intensity and ω_0 the laser frequency. The harmonic spectra is composed of two regions (i) one for photon energies below $3.17U_p + I_p$ (with I_p the ionization potential) is called plateau. It presents a rather constant yield as a function of harmonic order and (ii) harmonics having higher energies for which a fast yield decrease with increasing order is observed. The so-called harmonic cutoff energy then evolves linearly with the peak intensity I. The semi-classical description of HHG also allows for distinguishing two classes of trajectories in the plateau: the short and long trajectories named after their respective excursion time (from ionization to recombination) in the continuum [3]. The inherent process of HHG makes it a unique tool for ultrashort pulses generation (down to attoseconds) [4–6], time-resolved dynamics studies using the common pump-probe scheme [7–9] and molecular orbitals tomography ([10–12] and references therein).

Recent experimental investigations of HHG in solid targets showed drastically different behavior as compared to their gas counterparts. In particular, the evolution of the cutoff, which is expected to be proportional to the laser peak intensity (I), was measured to scale linearly with the electric peak amplitude of the drive laser (E) [13]. The experiments were performed using a ZnO crystal at a central frequency of 3.25μm. In [13] the authors model the HHG in solid by considering the classical motion on a single band and they showed that the calculated current could in principle exhibit the linear scaling of the harmonic cutoff with the amplitude of the electric field. The HHG in solid dielectrics distinguishes between the so-called intra- and interband ultrafast electron dynamics [14]. In [15–17], the authors non-ambiguously attributed the origin of HHG in a ZnO solid interacting with a laser of 3.76μm wavelength to interband process, while for longer wavelengths (THz regime) the intraband dynamics dominates when the harmonics slip below the band-gap energy [18, 19]. Intra- and interband mechanisms in HHG have been theoretically discriminated in [20] where the Houston states [21] basis has been used. The mechanisms underlying interband HHG are now well understood and in particular the dependence of the cutoff energy with the laser field amplitude has been extracted from semi-classical analysis [16] or solving the time-dependent Schrödinger equation [22]. Here it is worth noticing that the use of Wannier functions allows to assess the contribution of the lattice wells to the HHG interband processes [23]. In particular, it was demonstrated that the initial wave function, which is promoted to excited band, is experiencing a spread of the wave packet and finally has a chance to come back on the same Wannier state, which is the most likely process for low-order harmonics. In this work, we examine the HHG in bulk crystals assuming that single active electron processes dominate the HHG. We will concentrate more specifically on the contribution of intraband processes described using the Houston states which are themselves expanded on the basis of Wannier states [24]. The purpose of this Letter is to bring new physical insights into intraband process and to derive quantitative predictions of the HHG spectra features.

The laser-solid dynamics will be studied for linearly

polarized field. Consequently, as it is extensively done for atomic and molecular system with a good success, we will use a one-dimensional approach. The potential describing the target $V(x)$ is modeled by a spatial periodic function of periodicity a so that $V(x+a) = V(x)$. In the static view point, one obtains the different bands describing the system noted $\mathcal{E}_m(k)$ by solving the secular equation. Here, k is the wave vector which lies in the Brillouin zone given by $[-\pi/a, \pi/a]$ of the reciprocal lattice. The interband HHG induced by the laser interaction, excites to higher bands portion of the ground state wave packet as also identified for the photoemission in solids [25]. The intraband dynamics is described using the formalism presented in [20] employing the Houston states. The current associated with the intraband process on band m is given by [26]:

$$j_{rad}(t) = \frac{\partial \mathcal{E}_m(p)}{\partial p}\Big|_{p=k(t)} \tag{1}$$

with $k(t) = A(t)$ imposed by the spatial periodicity of the lattice and with $\mathcal{E}_m(p)$ being the relation dispersion of the band under consideration [27]. The vector potential $A(t)$ is related to the electric field by $E(t) = -\frac{\partial A(t)}{\partial t}$. In the case of a relation dispersion expressed as $\mathcal{E}_m(k) = \mathcal{E}_{m,0} + \mathcal{E}_{m,1} cos(ka)$ and a vector potential given by $A(t) = A_0 sin(\omega_0 t)$, the current is written:

$$j_{rad}(t) = -ia\mathcal{E}_{m,1} \sum_{oddn} J_n(\frac{\omega_B}{\omega_0}) e^{in\omega_0 t} \tag{2}$$

with n being an odd integer. J_n is the Bessel function of order n and ω_B is the Bloch frequency defined by $\omega_B = aE_0$. E_0 is the field amplitude which relates to the vector potential amplitude by $E_0 = A_0\omega_0$. The radiation is then composed of odd harmonics of the laser frequency. The yield of the n^{th} harmonic is given by $|a\mathcal{E}_{m,1} J_n(\frac{\omega_0}{\omega_B})|^2$. Despite the fact that an analytical expression of the amplitude of a given harmonic generated by an intraband process is obtained, a clear physical process is missing. In particular, processes such as recombination invoking energy conservation at a given momentum k cannot clearly be defined. Moreover this model do not provide a clear distinction between what could appear as a plateau and a cut-off. As importantly, it does not indicate the existence or the nonexistence of short and long trajectories as defined for atomic and molecular targets and more generally does not provide any time information.

The purpose of this work is to give a clear physical picture answering the previous questions. To do so Eq. (1) is reformulated by means of the Wannier state representation of the wave function. Despite the fact that Wannier states are not eigenstates of the field-free Hamiltonian, it is a convenient basis for the interpretation of well to well transitions. In the above cited work [23], the model is based on the SFA approach and used for describing the interband process. The full wave function is split into the contribution of an unperturbed ground state (using the Wannier expansion) and a continuum part associated to the upper band. Here we use the Wannier basis in order to express the adiabatically modified wave function of a given band to investigate the intraband harmonic process. The eigenstate defined by the band n under consideration for a given momentum k, noted $\varphi_{n,k}(x)$, is then given by [28]:

$$\varphi_{n,k}(x) = \sqrt{\frac{a}{2\pi}} \sum_l w^l(x) e^{ilka}, \tag{3}$$

with $w^l(x) = w(x - la)$ being the Wannier function of index l associated with the band n in the field-free case. Keeping in mind that the calculations refer to a single band n, $\varphi_{n,k}(x)$ will be noticed $\varphi_k(x)$ in the following. The Wannier function $w(x-la) = \sqrt{\frac{a}{2\pi}} \int_{BZ} dg \varphi_g(x) e^{-ilga}$ is a function of space localized on the site $x = la$. The integration is performed over the Brillouin zone (BZ). In [28], it has been shown that the Wannier function presents an exponential decrease of the amplitude of the wave function as $|x - la|$ becomes large. The current $j_{rad}(t)$ obtained on the Houston basis is given by $j_{rad}(t) =< \varphi_{k(t)}(x)|\hat{p}|\varphi_{k(t)}(x) >$ with $\hat{p}$ the momentum operator [20, 26]. Introducing the Wannier expansion of the Houston states, the current associated with the intraband HHG is given by:

$$j_{rad}(t) = \sum_{\Delta l} O_{\Delta l} e^{i\Delta l k_0 a} e^{i\Delta l a A(t)}, \tag{4}$$

where $O_{\Delta l} = \sum_l < w^{l+\Delta l}(x)|\hat{p}|w^l(x) >$ is the dipole matrix element between Wannier states which depends only on Δl and is a decreasing function of Δl. The $O_{\Delta l}$ coefficient can also be expressed by means of the dispersion relation. Therefore $O_{\Delta l}$ only depends on the structure of the band and thus can be viewed as a structural coefficient. k_0 is the initial momentum defined by the initial eigenstate. The Wannier states are the result of an integration over the whole Brillouin zone and are independent on k_0 which only affects the phase coefficient of the Bloch state expansion on the Wannier state. In particular, the dipole matrix elements do not depends on k_0. Hereafter, we choose $k_0 = 0$ for the sake of simplicity. Defining the vector potential $A(t) = A_0 sin(\omega_0 t)$ and using the Bessel expansion, one retrieves the expression of the current for a given harmonic order n:

$$\tilde{j}_{rad}(n) = \sum_{\Delta l} O_{\Delta l} J_n(\Delta l \frac{\omega_B}{\omega_0}). \tag{5}$$

This equation is a generalization of Eq. (2) for any dispersion relation of a given band. Alternatively, Eq. (5) can be expressed as follows:

$$\tilde{j}_{rad}(n) = \sum_{\Delta l} O_{\Delta l} \int dt e^{iS(t)}, \tag{6}$$

with $S(t) = -n\omega_0 t + \Delta l a A(t)$. $S(t)$ is assimilated to an action term. We note that this term is independent of the band considered and that the band structure impacts only the $O_{\Delta l}$ coefficient. This equation can be solved using the saddle point approximation leading to the saddle point condition $\frac{\partial S}{\partial t} = 0$ where the action phase remains stationary. The latter equation is re-casted as:

$$cos(\omega_0 t_s) = \frac{n\omega_0}{\Delta l \omega_B} = \gamma \tag{7}$$

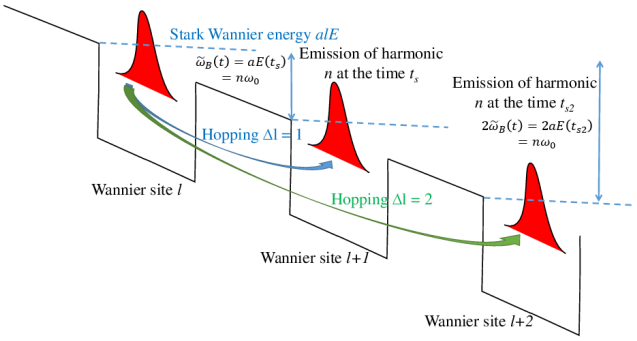

Figure 1. (Color online) Schematic of the physical process leading to intraband HHG. The hopping from well l to $l+1$ occurs at the time for which the diabatic Bloch frequency $\tilde{\omega}_B(t_s)$ equals the energy of harmonic n.

where $\omega_B = E_0 a$ is the Bloch frequency as defined earlier. Eq. (7) can also be written $\Delta l E_0 a cos(\omega_0 t_s) = \Delta l \tilde{\omega}_B(t_s) = n\omega_0$ which can be easily interpreted since the well of index l has a Stark shifted energy provided by the quantity $laE(t)$ in the presence of the field. If one considers the hopping from the well indexed by l to the neighbor well indexed by $l + \Delta l$, then the equation $\Delta l \tilde{\omega}_B(t_s) = n\omega_0$ corresponds to the energy conservation of the transition, where the instantaneous Bloch frequency $\tilde{\omega}_B(t_s) = E_0 a cos(\omega_0 t_s)$ is defined. The Figure (1) sketches this hopping process. Note that the hopping occurs for all wells at the same time, making the wells indistinguishable. Only the hopping process characterized by a given Δl can be discriminated in the HHG spectra. From Eq. (7), two regimes can be defined, (i) - when $\gamma < 1$ for which the saddle point solution t_s is real, and (ii) - when $\gamma > 1$ for which the saddle point solutions are purely imaginary. The regime transition occurs when $\gamma = 1$ corresponding to a threshold harmonic order given by $n_c = \frac{\Delta l \omega_B}{\omega_0}$. In Fig. (2) we show the harmonic spectra comparing the yield obtained from the saddle point analysis and using the analytical solution given by Eq. (5) based on the Bessel function expansion. The calculation have been performed so that $O_j = \delta_{j,\Delta_l}$ in order to get rid of the structural contributions and to discriminate the dynamics of the process.

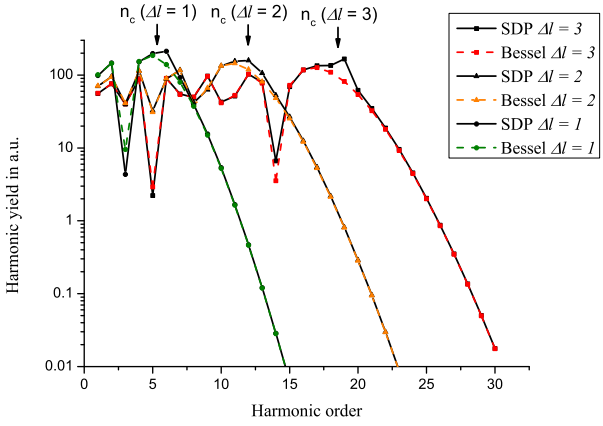

Figure 2. (Color online) Plot of the harmonic yield as a function of harmonic order. The laser condition are a peak intensity of 3.5 TW/cm^2, a central frequency of 4μm. The pulse is assumed infinite in time. The calculation have been performed by the saddle point analysis given by Eq.(7) (full black curve referred as SDP) and using the analytical formula given by Eq. (5)(color dashed curves). The hopping form the well l to $l+1$, $l+2$ and $l+3$ have been presented. Calculations have been performed for dispersion relation satisfying $O_j = \delta_{j,\Delta_l}$. The periodicity of the lattice $a = 8$ a.u. is chosen in order to mimic the spatial periodicity of the ZnO lattice.

An good agreement for the harmonic yield is obtained between the analytical solution and the saddle point analysis. As shown in the following, the saddle point analysis provides additional information such as scaling law of the HHG spectra features. When $\gamma > 1$ two purely imaginary saddle point solutions can be defined per half cycle and only one solution is physical (i.e. having a positive action) leading to an exponential decrease of the yield with increasing harmonic order. This is shown in Fig. (2) where an exponential decrease of the yield is observed for harmonic orders larger than the cut-off defined by $n_c = \frac{\Delta l \omega_B}{\omega_0}$. Note that the cut-off harmonic depends linearly on the electric field as experimentally observed in [13]. This is in contrast with the harmonic emission from atomic systems for which the harmonic cut-off depends linearly on the field intensity. The cut-off harmonic depends also linearly on the wavelength of the driving field as it was also observed from numerical analysis in [29]. We now examine more in detail the structure of the saddle point solution t_s defined by Eq. (7) when $\gamma > 1$. Since the real part of t_s is 0, the harmonics are all emitted at the maximum of the laser field. On the other hand when $\gamma < 1$ two solutions can be obtained leading to real action terms of opposite sign. As a consequence the yield can be defined by a cosine (or sine) function of the ac-

tion which exhibits an oscillatory behavior as a function of harmonic order as observed in Fig. (2).

In the context of isolated, short pulses generation two important features are at play. On one hand the yield from one harmonic to the next must remain rather constant and the emission time should also be steady from one harmonic to the next. HHG in solid satisfies the first requirement and we now investigate the emission time for intraband process. The time at which the harmonics are emitted depends on harmonic order and also of the hopping between the wells we are considering given by the value of Δl. In Fig. (3) we show the evolution of the emission time normalized to a phase $\omega_0 Re(t_s)$ as a function of harmonic order and also of Δl.

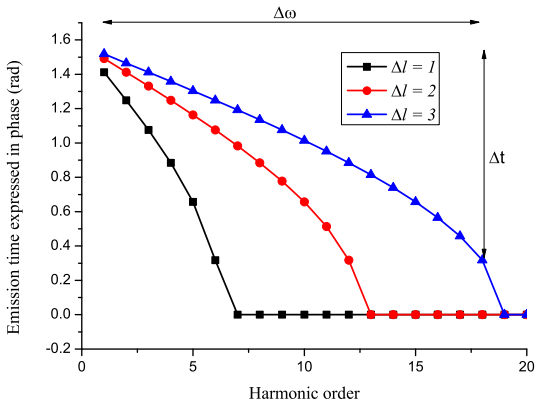

Figure 3. (Color online) Plot of the real part of the saddle point equation given by Eq. (7). The laser conditions are the same as the ones given in Fig. (2).

We note from the harmonics emission time, that harmonics belonging to the cut-off are all emitted in phase at the maximum of the electric field. This is in contrast with atomic and molecular case for which the recombination time close to the cut-off corresponding to the zero of the electric field. On the other hand the emission times of harmonics generated in the plateau are quite dispersed going from the phase $\pi/2$ (0 of the field) to 0 (maximum of the field). In particular, the lower harmonic orders are emitted close the 0 of the electric field which differs from atomic and molecular systems for which the phase spanned by the emission time is quite small (less than 0.3 rad) [30]. From our model we can extract the chirp associated to the intraband harmonic process. We can define this chirp as the ratio $\beta = \frac{\Delta t}{\Delta \omega} \approx \frac{\pi/2}{\omega_0^2 n_c} = \frac{\pi}{2\omega_0 \Delta l \omega_B}$ (see Fig. 3). This coefficient is then proportional to the ratio of the driving laser wavelength and electric field amplitude. Note that for atomic systems, this coefficient has been shown to be inversely proportional of the peak intensity [31]. Here it is worth noticing that our method, based on saddle point analysis, naturally leads to the time-frequency information for the whole harmonic spectrum. This is of particular interest since this information may be difficult to obtain using the usual Gabor or wavelet transforms, especially for low order harmonics [20].

Another feature which can be extracted from the saddle point analysis is the yield of the harmonics. It has been shown experimentally that the yield for rather low harmonics order follows the law I^n with n the harmonic order and I the peak intensity of the driving laser [13]. This scaling law is valid for harmonics belonging to the cut-off. For harmonics belonging to the plateau, experimental results show an increase of the yield proportional to the intensity. From our model, the harmonic yield can be obtained by the formula $W \propto exp(-2ImS_s)$, with S_s the action calculated at the saddle point [32, 33]. We then obtain an harmonic yield which follows the law I^n for harmonics in the cut-off. We also get a yield of ω_0^{-2n} for the dependences of the harmonics in the cut-off as a function of the central frequency of the driving laser. This is an interesting feature explaining why most of HHG in solid are observed for long wavelengths, which goes along with the fact that the resulting harmonics are not absorbed after the propagation threw few mono-layers of the solid. For harmonics generated in the plateau, the action S_s is purely real and the yield is independent on n, I and ω_0. The harmonic yield dependence as a function of Δl is more subtle to predict since it originates from two contributions. The first contribution comes from the overlap function $O_{\Delta l}$ which decreases with increasing Δl. The second contribution stems from the action and we show that the yield issued from the action is proportional to Δl^{2n}. These two effects go in opposite directions which makes the yield as a function of Δl a distribution depending on the band structure. Finally as it was stated in the introduction, the highest contribution of the interband HHG stems from $\Delta l = 0$ in contrast with intraband process which contribution is 0 for symmetry reasons.

In conclusion, we proposed to use the Wannier analysis for interpreting the physics of the intraband harmonic process. We have shown that an intraband harmonic process cannot simply be interpreted as transitions at a given k in the Brillouin zone as it was demonstrated for the interband transition. The Wannier picture is then necessary to invoke transition is space interpreted as hopping from one well to the neighbor wells. In particular we show that the intraband harmonic generation occurs when the diabatic Bloch frequency equals the energy of a harmonic photon. Using the saddle point analysis, we have shown that the cut-off harmonic, the yield as a function of intensity and central frequency of the driving laser reproduces the behavior observed experimentally for low order harmonics. We demonstrated that the contribution from band structure given by the dispersion relation, and the dynamics of the interaction can be disentangled. In particular we show that the dynamics is only driven by the periodicity of the lattice and by the laser parameters.

Finally the dependence of the yield to Δl, corresponding to the hopping between wells, is very different from inter- to intraband processes. The interband HHG shows a most likely contribution from $\Delta l = 0$ while intraband dynamics mostly involves transitions between different wells ($\Delta l \neq 0$). The intraband dynamics exhibits a cut-off which depends on Δl and each channel which can be studied independently then leading to band structure information.

We gratefully acknowledge fruitful discussions with P. Martin and J.C. Delagnes. F.C. would like to thank the PICS №36934 program from the CNRS. Computer time for this study was provided by the computing facilities MCIA (Mésocentre de Calcul Intensif Aquitain) of the Université de Bordeaux and of the Université de Pau et des Pays de l'Adour.

* fabrice.catoire@celia.u-bordeaux.fr

[1] P.B. Corkum. *Phys. Rev. Lett.*, 71:1994, 1993.
[2] B. Yand K.J. Schafer, L.F. Dimauro, and K.C. Kulander. *Phys. Rev. Lett*, 70:1599, 1993.
[3] M. Lewenstein, Ph. Balcou, M. Yu Ivanov, A. L'huillier, and P.B. Corkum. *Phys. Rev. A*, 49:2117, 1994.
[4] P. Agostini and L.F. DiMauro. *Rev. Mod. Phys.*, 67:813, 2004.
[5] F. Krausz and M. Ivanov. *Rev. Mod. Phys.*, 81:163, 2009.
[6] M. Chini, K. Zhao, and Z. Chang. *Nat. Phot.*, 8:178, 2014.
[7] W. Li, X. Zhou, R. Lock, S. Patchkovskii, A. Stolow, H. C. Kapteyn, and M. M. Murnane. *Science*, 322:1207, 2008.
[8] H. J. Wörner, J. B. Bertrand, B. Fabre, J. Higuet, H. Ruf, A. Dubrouil, S. Patchkovskii, M. Spanner, Y. Mairesse, V. Blanchet, E. Mével, E. Constant, P. B. Corkum, and D. M. Villeneuve. *Science*, 334:208, 2011.
[9] J. Caillat, A. Maquet, S. Haessler, B. Fabre, T. Ruchon, P. Salières, Y. Mairesse, and R. Taïeb. *Phys. Rev. Lett.*, 106:093002, 2011.
[10] J. Itatani, J. Levesque, D. Zeidler, H. Niikura, H. Pépin, P.B. Corkum J.C. Kieffer, and D.M. Villeneuve. *Nature*, 432:867, 2004.
[11] S. Haessler, J. Caillat, W. Boutu, C. Giovanetti-Teixeira, T. Ruchon, T. Auguste, Z. Diveki, P. Breger, A. Maquet, B. Carré, R. Taïeb, and P. Salières. *Nat. Phys.*, 6:200, 2010.
[12] C. Vozzi, M. Negro, F. Calegari, G. Sansone, M. Nisoli, S. De Silvestri, and S. Stagira. *Nat. Phys.*, 7:822, 2011.
[13] S. Ghimire, A.D. DiChiara, E. Sistrunk, P. Agostini, L.F. DiMauro, and D.A. Reis. *Nat. Phys.*, 7:138, 2011.
[14] D. Golde, T. Meier, and S. W. Koch. *Phys. Rev. B*, 77:075330, 2008.
[15] G. Vampa, T. J. Hammond, N. Thiré, B. E. Schmidt, F. Légaré, C. R. McDonald, T. Brabec, and P.B. Corkum. *Nature (London)*, 522:462, 2015.
[16] G. Vampa, T. J. Hammond, N. Thiré, B. E. Schmidt, F. Légaré, C. R. McDonald, T. Brabec, D. D. Klug, and P.B. Corkum. *Phys. Rev. Lett.*, 115:193603, 2015.
[17] G. Vampa, C.R. McDonald, G. Orlando, P.B. Corkum, and T. Brabec. *Phys. Rev. B*, 91:064302, 2015.
[18] M. Hohenleutner, F. Langer, O. Schubert, M. Knorr, U. Huttner, S.W. Koch, M. Kira, and R. Huber. *Nature*, 523:572, 2015.
[19] O. Schubert, M. Hohenleutner, F. Langer, B. Urbanek, C. Lange, U. Huttner, D. Golde, T. Meier, M. Kira, S. W. Koch, and R. Huber. *Nat. Phot.*, 8:119, 2014.
[20] M. Wu, S. Ghimire, D. A. Reiss, K. J. Schafer, and M. B. Gaarde. *Phys. Rev. A*, 91:043839, 2015.
[21] W. V. Houston. *Phys. Rev.*, 57:184, 1940.
[22] T. Ikemachi, Y. Shinohara, T. Sato, J. Yumoto, M. Kuwata-Gonokami, and K.L. Ishikawa. *Phys. Rev. A*, 95:043416, 2017.
[23] E. Osika, A. Chacón, L. Ortmann, N. Suárez, J.A. Pérez-Hernández, B. Szafran, M.F. Ciappina, F. Sols, A.S. Landsman, and M. Lewenstein. *Phys. Rev. X*, 7:021017, 2017.
[24] G. Wannier. *Phys. Rev.*, 52:191, 1947.
[25] F. Catoire and H. Bachau. *Phys. Rev. Lett.*, 115:163602, 2015.
[26] N.W. Aschcroft and N.D. Mermin. *Solid State Physics*. Cengage Learning, Boston, 1976.
[27] J.B. Krieger and G.J. Iafrate. *Phys. Rev. B*, 33:5494, 1986.
[28] W. Kohn. *Phys. Rev.*, 115:809, 1959.
[29] M. Wu, D. A. Browne, K. J. Schafer, and M. B. Gaarde. *Phys. Rev. A*, 94:063403, 2016.
[30] D. Shafir, H. Soifer, B.D. Bruner, M. Dagan, Y. Mairesse, S. Patchkovskii, M. Yu. Ivanov, O. Smirnova, and N. Dudovich. *Nature*, 485:343, 2012.
[31] G. Doumy, J. Wheeler, C. Roedig, R. Chirla, P. Agostini, and F.F. DiMauro. *Phys. Rev. Lett.*, 102:093002, 2009.
[32] T. Auguste, F. Catoire, P. Agostini, L.F. DiMauro, C.C. Chirila, V.S. Yakovlev, and P. Salières. *New Journal of Physics*, 14:103014, 2012.
[33] L.D. Landau and E.M. Lifshitz. *Quantum Mechanics*. 3rd edn (Oxford: Pergamon), 1977.